Journal of Alloys and Compounds 572 (2013) 1–4

Contents lists available at SciVerse ScienceDirect

Journal of Alloys and Compounds

journal homepage: www.elsevier.com/locate/jalcom

# Low-field induced large reversible magnetocaloric effect in $Tm_3Co$ compound

Zhao-Jun Mo [a,b], Jun Shen [a,*], Li-Qin Yan [c], Jian-Feng Wu [a], Cheng-Chun Tang [b], Bao-Gen Shen [c]

[a] Key Laboratory of Cryogenics, Technical Institute of Physics and Chemistry, Chinese Academy of Sciences, Beijing, China
[b] School of Material Science and Engineering, Hebei University of Technology, Tianjin, China
[c] State Key Laboratory of Magnetism, Beijing National Laboratory for Condensed Matter, Physics and Institute of Physics, Chinese Academy of Sciences, Beijing, China

ARTICLE INFO

*Article history:*
Received 5 January 2013
Received in revised form 6 March 2013
Accepted 11 March 2013
Available online 6 April 2013

*Keywords:*
Magnetocaloric effect
$Tm_3Co$ compound
Magnetic entropy change
Refrigerant capacity power
Magnetic refrigeration

ABSTRACT

A large reversible magnetocaloric effect has been observed in $Tm_3Co$ compound. The $Tm_3Co$ compound exhibits two successive magnetic transitions with the increasing temperature: antiferromagnetic (AFM) to ferromagnetic (FM) transition at 4.5 K and FM to paramagnetic (PM) transition at 6.5 K. Under a magnetic field change of 5 T, the maximum value of magnetic entropy change $-\Delta S_M$ is 19.9 J/kg K at 7.5 K and the refrigerant capacity power (RCP) is 300 J/kg with no hysteresis loss. In particular, the large reversible $-\Delta S_M$ (11.6 J/kg K) is achieved for a low magnetic field change of 2 T. The large reversible magnetocaloric effect (both the large $-\Delta S_M$ and the high RCP) indicates that $Tm_3Co$ could be a promising candidate for magnetic refrigeration.



## 1. Introduction

Magnetic refrigeration is becoming a promising and viable technology for cryogenic applications. It is anticipated that the magnetic refrigeration is better than conventional vapor compression refrigeration, which has a lot of advantages such as high efficiency, energy saving and pollution-free [1]. Magnetic refrigeration is based on magnetocaloric effect (MCE), which is defined as the thermal response of a magnetic material to an applied field. It is necessary to explore advanced magnetic refrigerant materials with a large magnitude of isothermal magnetic entropy change ($\Delta S_M$) and/or adiabatic temperature change ($\Delta T_{ad}$) for practical application [2]. Up to now, many magnetic materials with high magnetocaloric performances have been found, such as $ErCo_2$ [3], $LaFe_{13-x}Si_x$ [4,5], $MnAs_{1-x}Sb_x$ [6], $MnFeP_{0.45}As_{0.55}$ [7] and $Gd_5Si_2Ge_2$ [8,9], etc. However, most of them are associated with the first-order magnetic or structural phase transition. The first-order transition is usually accompanied by a considerable thermal or magnetic hysteresis, which is disadvantageous for a magnetic refrigeration cycle [10–15]. Additionally, if a sufficient MCE of material can be achieved upon application of low magnetic fields (e.g., less than 2 T), it is feasible to design a refrigeration cycle using permanent magnets as the magnetic field source. Therefore, it is desirable to search for materials exhibiting a large MCE under low field ($\Delta H \leqslant 2$ T) with negligible thermal and field hysteresis loss, such as $ErMn_2Si_2$ [16], $GdNi_4M$ (M = Al, Si) [17], $PrMn_{1.4}Fe_{0.6}Ge_2$ [18], $TbCo_3B_2$ [19], $ErRu_2Si_2$ [20] and DyCuSi [21].

The binary $R_3Co$ system has a low-symmetry orthorhombic $Fe_3C$-type structure (Pnma space group) [22]. Rare earth atoms occupy two nonequivalent positions, 4c (*R*4*c*) and 8d (*R*8*d*). The atoms of 3*d* transition metal are located at the 4c position within the trigonal prisms formed by rare earth atoms. $R_3Co$ has the highest concentration of rare earth in such binary intermetallic system. It exhibits a complicated magnetic behavior including the field-induced magnetic phase transition and a substantial magnetocaloric effect [23,24]. Recently, the MCEs of $Tb_3Co$, $Er_3Co$ and $Gd_3Co$ compounds have been investigated with the maximal values of $-\Delta S_M$: 18, 17 and 11 J/kg K for a field change of 0–5 T, respectively [25–27]. In the present work, we report a large reversible MCE in $Tm_3Co$ compound. The maximum value of $-\Delta S_M$ is 19.9 J/kg K with the RCP (300 J/kg) for a field change of 0–5 T. It is noteworthy that a large $-\Delta S_M$ and RCP are achieved for a low magnetic field change of 0–2 T at 6.5 K, which make it attractive for application in low temperature magnetic refrigeration such as hydrogen liquefaction.

## 2. Experiments

The polycrystalline sample of $Tm_3Co$ compound was synthesized by arc melting of stoichiometric amounts of the elements Tm metals (99.9%) and Co (99.9%) under a purified argon atmosphere on a water-cooled copper hearth using a titanium zirconium alloy as a getter (The content of Tm was 3% more than the theoretical value). The ingot was melted for three times with the button being turned over after

* Corresponding author.
*E-mail address:* jshen@mail.ipc.ac.cn (J. Shen).

0925-8388/$ - see front matter © 2013 Elsevier B.V. All rights reserved.
http://dx.doi.org/10.1016/j.jallcom.2013.03.109

each melting to ensure the homogeneity. The sample was annealed at 1123 K for 10 days, and a subsequent quenching to room temperature was performed to obtain crystalline samples. Powder X-ray diffraction (XRD) measurement was performed at room temperature by using Cu Kα radiation to identify the crystal structure and the lattice parameters. Magnetizations were measured by employing a commercial superconducting quantum interference device (SQUID) magnetometer, model MPMS-7 from Quantum Design Inc.

## 3. Results and discussion

Fig. 1 shows the Rietveld refined powder XRD pattern of $Tm_3Co$ compound at room temperature. The refinement result shows that the prepared sample is of single phase, crystallizing in the orthorhombic $Fe_3C$ type crystal structure [space group Pnma (62)]. Tm atoms occupy two nonequivalent positions [4c (*R*4*c*) and 8d (*R*8d)] and Co atoms are located at the 4c position within the trigonal prisms formed by Tm atoms. Results of all the structural parameters are determined by the Rietveld technique using GSAS program and summarized in Table 1.

The zero-field-cooling (ZFC) and field-cooling (FC) temperature dependences of magnetizations for $Tm_3Co$ compound are shown in Fig. 2a under a low magnetic field of 0.01 T. It can be seen that there is almost no thermal hysteresis between the ZFC and FC curves when the temperature increases above 6.5 K. The small bifurcation may be related to the domain-wall pinning effect below 6.5 K. The d*M*/d*T* versus *T* curve (the inset of Fig. 2a) reveals that the $Tm_3Co$ has an AFM to FM transition at $T_N$ = 4.5 K and a FM to PM transition at $T_C$ = 6.5 K, which is corresponding to the minimum value of d*M*/d*T*. Fig. 2a also indicates that the magnetic susceptibility of the $Tm_3Co$ compound above 7 K follows the Curie–Weiss law $\chi_m^{-1} = (T-\theta_p)/C_m$, where $\theta_p$ is the paramagnetic Curie temperature and $C_m$ is the Curie–Weiss constant. The value of $\theta_p$ for $Tm_3Co$ is positive and equals to 3.5 K. The effective magnetic moment $\mu_{eff}$ per Tm atom (7.71 $\mu_B$) is obtained based on the value of $C_m$, which is slightly larger than 7.56 $\mu_B$ for the free $Tm^{3+}$ ion [28]. Previous studies have shown that due to the filling of 3d band of Co by 6s and 5d electrons of R atoms, the Co sublattice is nearly nonmagnetic; however, the partial polarization of 3d band by the rare earth exchange field can lead to small moment at the Co site. Such an excess of $\mu_{eff}$ has been observed in $Er_3Co$ compound [29]. Therefore, the additional contribution of the effective magnetic moment should be attributed to a part of Co $3d^8$-electrons. Fig. 2b shows the temperature dependences of the magnetization for $Tm_3Co$ in different magnetic fields. It clearly shows that the magnetization below $T_N$ increases greatly and eventually reach to a plateau at $\mu H$ = 0.7 T with increasing field, indicating a field-induced metamagnetic transition from AFM to FM. When the applied magnetic field is 0.2 T, *M*–*T* curves clearly show an AFM to FM transition and a FM to PM transition with increasing temperature in $Tm_3Co$ compound. When the applied magnetic field is higher than ~0.5 T, *M*–*T* curve shows only one magnetic transition from FM–PM due to the suppression of AFM states.

**Table 1**
Structural parameters for $Tm_3Co$ refined from XRD data with $R_P$ = 4.7% and $R_{WP}$ = 6.6%.

| Lattice parameters (Å) | Coordinates of atoms (*x*, *y*, *z*) | Shortest interatomic distances (Å) | |
|---|---|---|---|
| *a* = 6.8635 | $Tm_1$ (0.1830, 0.0623, 0.1683) | $Tm_1$–$Tm_1$ 3.3937 | $Tm_1$-Co 2.7080 |
| *b* = 9.0895 | $Tm_2$ (0.0397, 0.2500, 0.6305) | | |
| *c* = 6.1277 | Co (0.3974, 0.2500, 0.4561) | | |

The isothermal magnetization curves as a function of magnetic field are measured in applied fields up to 5 T, in a temperature range of 2–30 K, as shown in Fig. 3a. The data were acquired in the processes of increasing and decreasing fields, respectively. The *M* (*H*) isotherms do not exhibit magnetic hysteresis, implying that this compound is a soft ferromagnetic. As is well known, no hysteresis in magnetization as a function of both temperature and magnetic field is indispensable for a reversible MCE. The magnetization of $Tm_3Co$ below $T_N$ increases linearly with increasing magnetic field in low-field ranges, indicating the existence of AFM ground state. However, when the applied field exceeds 0.4 T, the magnetization exhibits a sharp increase, which indicates that the field-induced metamagnetic transition from AFM to FM state occurs. Eventually, the AFM state is driven into the FM one

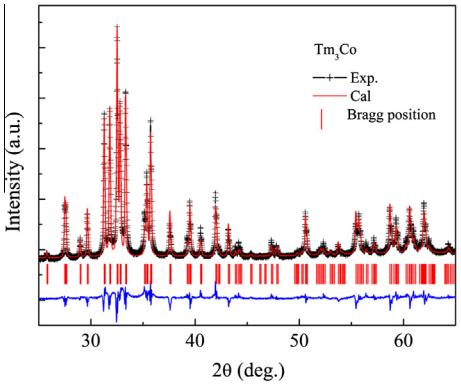


**Fig. 1.** Rietveld refined powder XRD patterns of $Tm_3Co$ compound at room temperature.

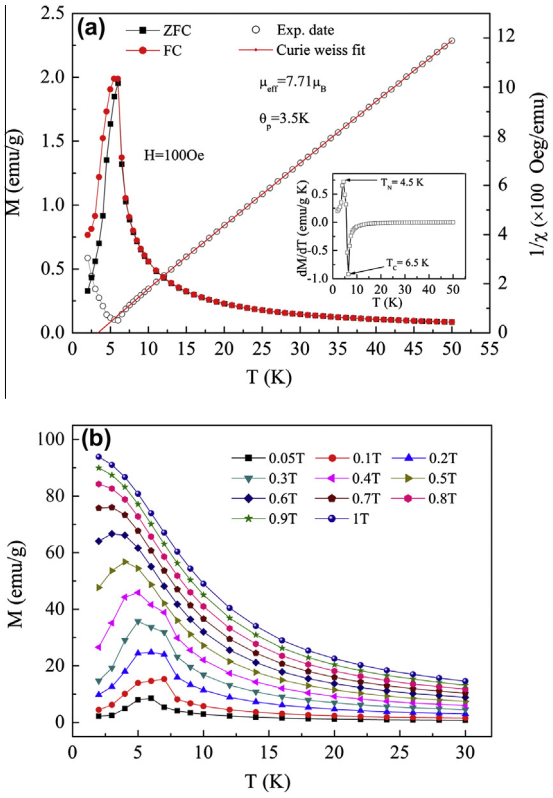


**Fig. 2.** (a) Temperature dependences of ZFC and FC magnetizations under 0.01 T and the temperature variation of the ZFC inverse susceptibility fitted to the Curie–Weiss law. The insets show the d*M*/d*T*–*T* curve. (b) Temperature dependences of the magnetization under different magnetic fields.

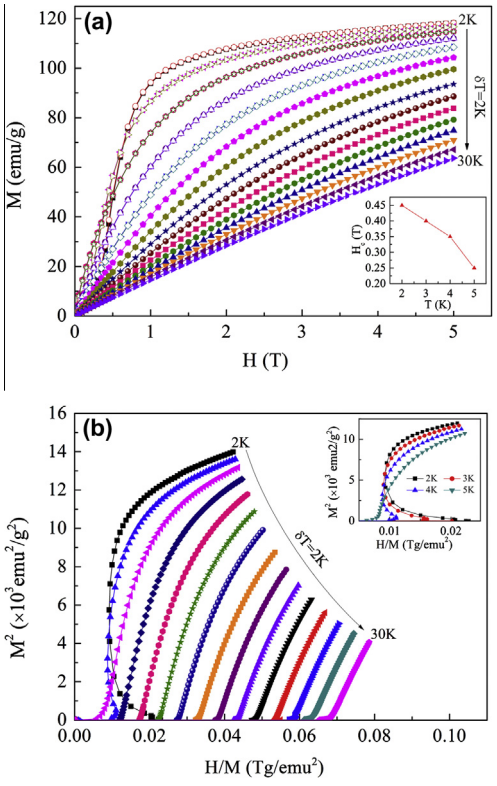


**Fig. 3.** (a) Isothermal magnetization curves of $Tm_3Co$ compound; Inset: the temperature dependence of the critical magnetic field; and (b) the Arrott plots of $Tm_3Co$ compound in the temperature range of 2–30 K. The inset of (b) shows the magnified Arrott plots at 2, 3, 4, 5 K.

as the magnetic field reaches about 1 T. The critical magnetic field ($H_c$) from AFM to FM states is determined from the local maximum point of the d$M$/d$H$ (at 2, 3, 4 and 5 K) curves. The $H_c$ increases monotonically with the decrease of temperature and reaches a value of 0.45 T at 2 K (see the inset of Fig. 3a). It reveals that the $Tm_3Co$ compound is a weak antiferromagnet and the AFM structure could be easily destroyed and enter to FM state by a small magnetic field below $T_N$. Meanwhile, it implies the dominant fraction of FM than that of AFM state after the field-induced metamagnetic transition. Fig. 3b shows the Arrott plots of $Tm_3Co$ compound in the temperature range of 2–30 K. As is well known, the negative slope of Arrott plot implies a first-order magnetic transition, while a positive slope indicates a second-order transition [30]. Herein the Arrott plot of $Tm_3Co$ exhibits a negative slope below $T_N$ (the inset of Fig. 3b), which further confirms a first-order magnetic transition

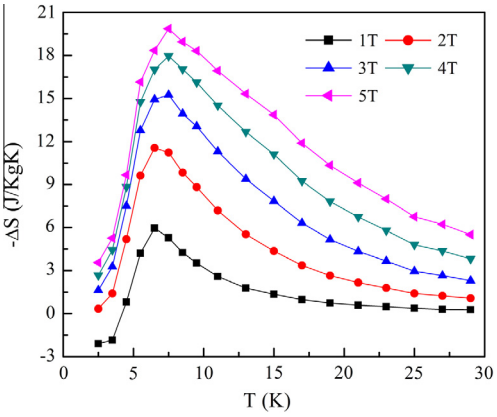


**Fig. 4.** Temperature dependences of magnetic entropy change for different magnetic field changes of 1, 2, 3, 4, 5 K.

from AFM to FM. However, the positive slope of the plots is observed above $T_N$, which indicates the characteristic of field-induced second-order from FM to PM magnetic transition. Similar result has also been observed in $Ho_3Co$ [31].

The magnetic entropy change $-\Delta S_M$ for $Tm_3Co$ is calculated from isothermal magnetization data (see Fig. 3a) by using the Maxwell relation $\Delta S(T,H) = \int_0^H (\partial M/\partial T)_H dH$. The temperature dependences of $-\Delta S_M$ calculated from magnetizations for different field changes are shown in Fig. 4. The maximum value of $-\Delta S_M$ is found to increase monotonically with the increase of applied magnetic field and reaches a value of 19.9 J/kg K for a magnetic field change from 0 to 5 T. Particularly, the maximum value of -$\Delta S_M$ is found to be 11.6 J/kg K under a low magnetic change of 2 T, which can be realized by permanent magnet and be advantageous for applications. The large $-\Delta S_M$ results from the field-induced metamagnetic transition of AFM–FM in $Tm_3Co$, which is similar to $ErRu_2Si_2$ [20]. Moreover, the $-\Delta S_M$ does not die out even at temperatures well above $T_c$, possibly due to the presence of spin fluctuations [26]. RCP is considered to be another important requirement of a potential magnetic refrigerant. It is a measure that how much heat can be transferred between the cold and hot sinks in one ideal refrigerant cycle [32]. The RCP value can be calculated by using a method for conventional refrigerant materials, as follows [33], RCP = $-\Delta S_M^{max}\ \delta T$. Here the $-\Delta S_M^{max}$ is the maximum magnetic entropy change, $\delta T$ is the full width of half maximum $-\Delta S_M^{max}$ in the magnetic field changes, respectively. Consequently, the RCP values of $Tm_3Co$ are calculated to be 300 and 93 J/kg for the magnetic field changes of 5 and 2 T, respectively. The large value of $-\Delta S_M$, the considerable RCP and no thermal as well as magnetic hysteresis loss make $Tm_3Co$ compound become a promising candidate for its application in magnetic refrigeration, such as helium and hydrogen liquefaction.

## 4. Conclusions

In conclusion, the polycrystalline $Tm_3Co$ intermetallic compound with a single phase has been synthesized and the magnetic and MCE properties have been studied. The compound exhibits two successive magnetic transitions: first-order transition from AFM to FM and second-order transition from FM to PM with increasing temperature. A large MCE without thermal and magnetic hysteresis loss is observed in $Tm_3Co$, which originates from the field-induced metamagnetic transition of AFM–FM. The values of $-\Delta S_M^{max}$ and RCP are 19.9 J/kg K and 300 J/kg for a field change of 0–5 T, respectively. In particular, for the relative low magnetic-field changes of 0–2 T, the $-\Delta S_M^{max}$ and RCP values are 11.6 J/kg K and 93 J/kg, which is important for the practical application of the $Tm_3Co$ compound in low-temperature. The present results indicate that the $Tm_3Co$ compound is expected to have effective applications in low temperature magnetic refrigeration.

## Acknowledgements

This work was supported by the National Basic Research Program of China (No. 2011AA03A404), the National Natural Science Foundation of China (Nos. 11004204; 11104337 and 51271192), and the Knowledge Innovation Project of the Chinese Academy of Sciences.

## References

[1] K.A. Gschneidner Jr., V.K. Pecharsky, A.O. Tsokol, Rep. Prog. Phys. 68 (2005) 1479.
[2] E. Brück, O. Tegus, D.T.C. Thanh, K.H.J. Buschow, J. Magn. Magn. Mater. 310 (2007) 2793.
[3] A. Giguere, M. Foldeaki, W. Shcnelle, E. Gmelin, J. Phys.: Condens. Matter 11 (1999) 6969.

[4] F.X. Hu, B.G. Shen, J.R. Sun, Z.H. Chen, G.H. Rao, X.X. Zhang, Appl. Phys. Lett. 78 (2001) 3675.
[5] F. Wang, Y.F. Chen, G.J. Wang, B.G. Shen, J. Phys. D: Appl. Phys. 36 (2003) 1.
[6] O. Tegus, E. Brück, K.H.J. Buschow, F.R. de Boer, Nature 415 (2002) 150.
[7] H. Wada, Y. Tanabe, Appl. Phys. Lett. 79 (2001) 3302.
[8] V.K. Pecharsky, K.A. Gschneidner Jr., Phys. Rev. Lett. 78 (1997) 4494.
[9] J.H. Belo, A.M. Pereira, J. Ventura, G.N.P. Oliveira, J.P. Araújo, P.B. Tavares, L. Fernandes, P.A. Algarabel, C. Magen, L. Morellon, M.R. Ibarra, J. Alloys Comp. 529 (2012) 89–95.
[10] M.H. Phan, G.T. Woods, A. Chaturvedi, S. Stefanoski, G.S. Nolas, H. Srikanth, Appl. Phys. Lett. 93 (2008) 252505.
[11] O. Tegus, E. Bruck, K.H.J. Buschow, F.R. De Boer, Nature (London) 415 (2002) 150.
[12] S. Gama, A. de Campos, A.A. Coelho, C.S. Alves, Y. Ren, F. Gacia, D.E. Brown, L.M. da Silva, A.M.G. Carvalho, F.C.G. Gandra, A.O. dos Santos, L.P. Cardoso, P.J. von Ranke, Adv. Funct. Mater. 19 (2009) 942.
[13] J.D. Zou, B.G. Shen, B. Gao, J. Shen, J.R. Sun, Adv. Mater. 21 (2009) 693.
[14] N.A. de Oliveira, P.J. von Ranke, Phys. Rep. 489 (2010) 89.
[15] V. Provenzano, A.J. Shapiro, R.D. Shull, Nature (London) 429 (2004) 853.
[16] L. Li, K. Nishimura, W.D. Hutchison, Z. Qian, D. Huo, T. Namiki, Appl. Phys. Lett. 100 (2012) 152403.
[17] T. Toliński, M. Falkowski, K. Synoradzki, A. Hoser, N. Stüßer, J. Alloys. Comp. 523 (2012) 43–48.
[18] R. Zeng, S.X. Dou, J.L. Wang, S.J. Campbell, J. Alloys Comp. 509 (2011) 119–123.
[19] L. Li, D. Huo, H. Igawa, K. Nishimura, J. Alloys. Comp. 509 (2011) 1796–1799.
[20] T. Samanta, I. Das, S. Banerjee, Appl. Phys. Lett. 91 (2007) 152506.
[21] J. Chen, B.G. Shen, Q.Y. Dong, F.X. Hu, J.R. Sun, Appl. Phys. Lett. 96 (2010) 152501.
[22] D.T. Cromer, A.C. Larson, Acta Crystallogr. 14 (1961) 1226.
[23] A.F. Gubkin, A. Podlesnyak, N.V. Baranov, Phys. Rev. B 82 (2010) 012403.
[24] N.V. Baranov, E. Bauer, R. Hauser, A. Galatanu, Y. Aoki, H. Sato, Eur. Phys. J. B 16 (2000) 67.
[25] B. Li, J. Du, W.J. Ren, W.J. Hu, Q. Zhang, D. Li, Z.D. Zhang, Appl. Phys. Lett. 92 (2008) 242504.
[26] P. Kumar, N.K. Singh, A.K. Nayak, A. Haldar, K.G. Suresh, A.K. Nigam, J. Appl. Phys. 107 (2010) 09A932.
[27] S.K. Tripathy, K.G. Suresh, A.K. Nigam, J. Magn. Magn. Mater. 306 (2006) 24–29.
[28] S. Baran, D. Kaczorowski, A. Arulraj, B. Penc, A. Szytuła, J. Magn. Magn. Mater. 323 (2011) 833–837.
[29] O.A.W. Strydom, L. Alberts, J. Less-Common Met. 22 (1970) 503.
[30] S.K. Banerjee, Phys. Lett. 12 (1964) 16.
[31] J. Shen, J.F. Wu, J. Appl. Phys. 109 (2011) 07A931.
[32] B.G. Shen, J.R. Sun, F.X. Hu, H.W. Zhang, Z.H. Chen, Adv. Mater. 21 (2009) 4545.
[33] K.A. Gschneidner Jr., V.K. Pecharsky, Annu. Rev. Mater. Sci. 30 (2000) 387.